International Journal of Heat and Mass Transfer 97 (2016) 596–602

Contents lists available at ScienceDirect

International Journal of Heat and Mass Transfer

journal homepage: www.elsevier.com/locate/ijhmt

Mathematical modelling of turbulent flow for flue gas–air Chevron type plate heat exchangers

Leila Vafajoo [a], Karim Moradifar [a], S. Masoud Hosseini [a,b], B.H. Salman [c,*]

[a] Department of Chemical and Environmental Engineering, Faculty of Engineering, I. Azad University, South Tehran Branch, Tehran, Iran
[b] Chemical Engineer in the Residue Fluidized Catalytic Cracking (RFCC) Unit, IKORC, Arak, Iran
[c] Department of Mechanical Engineering, University of Nevada, Las Vegas, NV 89154, USA

ARTICLE INFO

Article history:
Received 15 December 2015
Received in revised form 11 February 2016
Accepted 11 February 2016
Available online 1 March 2016

Keywords:
Mathematical modeling
Flue gas
Energy recovery
Recuperative heat exchanger

ABSTRACT

A mathematical model of a plate recuperative heat exchanger was developed in order to recover energy for refinery flue gases and preheating of the inlet air of a combustion chamber. Two-dimensional, compressible and turbulent flow conditions were undertaken. After the model verified, the results revealed that, replacing flat plate to Chevron-type plates led to major changes through the velocity vectors into the angular and eddy forms. Moreover, as the Chevron angle increased, more pronounced changes observed in the velocity vectors. Also it was revealed that, a five folds enhancement in the Reynolds number led to increasing of the corresponding Nusselt number and the pressure drop while lowering the Fanning friction factor. The bigger angle of the Chevron type plates resulted in 18% enhancement in the output air temperature as well as; an increase in the resulting flue gas pressure drop of 63% in comparison with the plate heat exchanger.

1. Introduction

The ever increasing demand for the reduction of energy costs has highlighted the role of the heat exchanger efficiency in the design of such equipment. One of the most applicable heat exchangers utilised widely in various industries is the plate configuration. In these heat exchangers (HEs), a number of plates placed between cold and hot fluids acting as a medium to transfer the energy of the latter to the former. It is thus; expected the plate geometry to play an effective role in enhancement of heat transfer rate and pressure drop [1–9]. Owing to the importance of this subject, in recent years numerous research activities done toward developing a mathematical model or empirical correlations for the fanning factor and Nusselt number of this types of plate heat exchangers (PHEs). Nevertheless, an exact or useful expression has not been provided over a wide range of the Reynolds number, geometrical shape or service fluid to date. Thus, it is not a sure bet that, an expression developed under certain conditions would fit other situations as well. On the other hand, most researches done upon the plate heat exchangers to date were related to the experimental design of this equipment for the water–air (liquid–gas) or water–water (liquid–liquid) flow [2,10].

In the present work, modelling of a one-pass plate heat exchanger for the flue gas–air system was performed. The heat transfer rate as well as; pressure drop of fluids were investigated for a flat and two different angles of Chevron plates. Moreover, the influence of the plate geometry on the heat transfer rate and pressure drop were studied for the turbulent regime. For prediction of the turbulent flow behaviour, a realisable K–ε model was utilised. This model was proposed previously when investigating the turbulence in the plate heat exchangers and led to more accurate results in comparison with other theoretical models of turbulent flow [11]. Furthermore, the design and operating data of the Tehran refinery flue gas utilized for modelling of the systems undertaken in this work. It is noteworthy that, in order to avoid the corrosion problems due to the 700 ppm concentration of the total sulphur content existed in the flue gas, it was indeed necessary to adjust the heat transfer rate such that, the operation temperature would be held above the flue gas sulphuric acid dew point [12,13].

2. Modelling

2.1. Theoretical backgrounds

In the plate heat exchangers the mass flow rate usually calculated by multiplying the velocity of the fluid into the flow direction by the cross sectional area perpendicular to the flow. This velocity

* Corresponding author. Tel.: +1 (702) 505 2935.
E-mail address: eng.bassam2007@yahoo.com (B.H. Salman).

http://dx.doi.org/10.1016/j.ijheatmasstransfer.2016.02.035
0017-9310/

Nomenclature

Roman symbols

A_{in}	inlet flow area (m^2)
A_C	cross sectional area of channel (m^2)
b	inter-plates distance (m)
c_p	heat capacity at constant pressure (J/kg K)
D_H	hydraulic diameter of channel (m)
f	friction factor
h	heat transfer coefficient (W/m^2 K)
I	turbulence intensity parameter
k	thermal conductivity (W/m K)
L	length of channel (m)
m	constant
n	constant
Nu	Nusselt number
P_x	corrugation pitch in the flow direction (m)
ΔP	pressure drop of channel (Pa)
Pr	prandtl number
q''	local heat flux (W/m^2)
Re	Reynolds number
T_{fluid}	temperature of the fluid (K)
T_{plate}	temperature of the plate wall (K)
$\overline{u}$	actual velocity (m/s)
U_{eff}	effective fluid velocity (m/s)
U_{in}	inlet fluid velocity (m/s)
u_{avg}	average velocity (m/s)
V	gas volume (m^3)
W	mass flow rate (kg/s)

Greek symbols

β	Chevron's angle (°)
ρ	Fluid density (kg/m^3)
μ	Fluid dynamic viscosity (kg/m s)

referred to as the effective velocity actually being the projection of the normal velocity. The inlet flow area was given as follows:

$$A_{in} = b.P_x \quad (1)$$

In which A_{in} was the inlet flow area, b was the inter-plates distance and the P_x was the corrugation pitch in the main flow direction.

Thus, the mass flow rate (W) was obtained by the following equation:

$$W = \rho.b.P_x.u_{eff} = \rho.b.u_{in}/Cos\beta \quad (2)$$

where β was the Chevron's angle. In addition, the cross sectional area (A_C) perpendicular to the flow direction was calculated as:

$$A_C = b.P_x/Cos\beta = 2b.P_x.Sin\beta/Sin2\beta \quad (3)$$

Moreover, the Fanning friction factor calculated as follows [14] and [15]:

$$f = (\Delta P/L).(D_H/2\rho u^2) \quad (4)$$

In which ΔP was the pressure drop and L and D_H were the length and hydraulic diameter of channel; respectively. In order to determine the heat transfer rate at different distances of plates, a local Nusselt number was defined as:

$$q'' = h(T_{plate} - T_{fluid}) \quad (5)$$

Where the q'' was the local values of the heat flux, and T_{fluid} and T_{plate} were temperature of the fluid and the plate wall; respectively. Finally the Nusselt number was calculated as follows:

$$Nu = h.D_H/k = (q''/(T_{plate} - T_{fluid})).(D_H/k) \quad (6)$$

Due to certain shape of plates, the flow pattern was turbulent hence; the energy transfer rate might have been calculated according to the Dittus–Boeller equation recommended for turbulent flow [16].

$$Nu = mRe^n Pr^{0.33} \quad (7)$$

$$Re = \rho.u_{eff}.D_H/\mu \quad (8)$$

$$Pr = C_P.\mu/k \quad (9)$$

In which, m and n were constants depending upon the flow regime and geometrical characteristics of the HE plates (*e.g.*; the corrugation angle) determined experimentally.

2.1.1. Physical parameters of streams

Since in the present system the passing streams through plates were gas–gas and the temperature gradient occurred, the system might be considered compressible. However, the density variations were calculated through the ideal gas law. This was rationalized due to the high operating temperatures (around 600 K) and medium pressures utilised. For calculation of viscosity of air and flue gases, the Sutherland relationship as well as; the kinetic theory of gases was respectively employed. In addition, the heat capacity and conduction heat transfer coefficient were calculated by the kinetic theory of gases.

2.2. Model geometry

2.2.1. Geometrical considerations

For the geometry establishment in the present model for the flat (P1) and Chevron models (P2 and P3), the dimensions of the industrial heat exchanger utilized provided by the TM20 model of the α-Laval company and presented in Table 1.

2.3. Model details and plate meshes

The numerical analysis procedure is dynamic modelling. Through considerations of the geometrical surfaces and overall heat transfer area as well as; the inlet and outlet HE headers, the effective length of the heat transfer for modelling was approximately determined to be 1000 mm. Plate thickness and the distance between them were selected to be 0.8 and 6 mm; respectively. In addition, the flat and Chevron plates were meshed by using square and triangular meshes; respectively. In order to obtain more accurate results, the effect of molecular viscosity near the walls was considered by implementing smaller mesh values in that vicinity. Figs. 1–3 displayed the meshes of flat and Chevron plates. The number of cells, faces and nodes for low and high meshes of the aforementioned three models were presented in Table 2. It was observed that, at both low and high ends of the

Table 1
Geometry parameters of models.

Model	b (mm)	P_x (mm)	Chevron angle (°)
P1	Flat plate		–
P2	1.9	10	29
P3	3.8	10	85

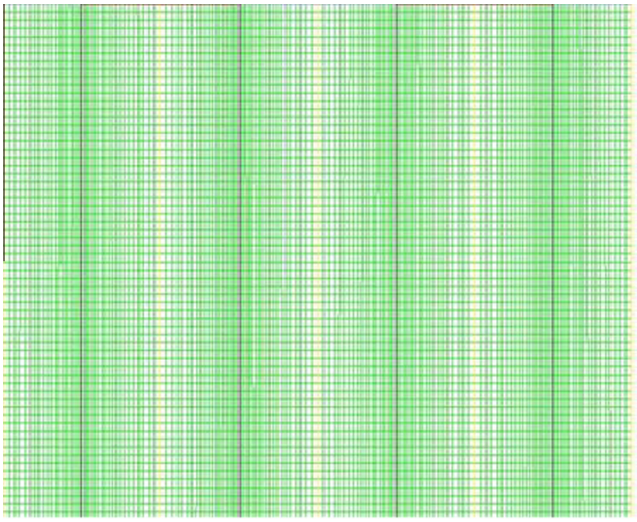

Fig. 1. The square meshes of the P1 model.

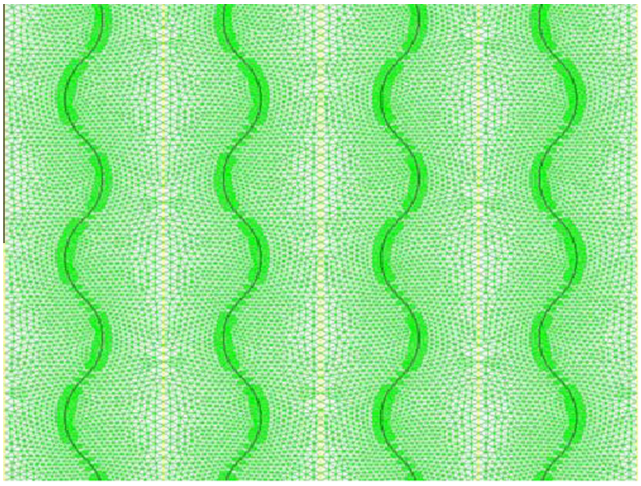

Fig. 2. The triangular meshes of the P2 model.

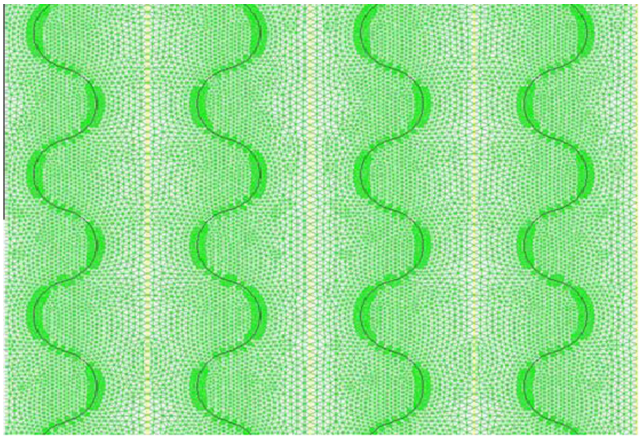

Fig. 3. The triangular meshes of the P3 model.

mesh sizes, the temperature changed at both sides of plates (in all cases considered) only within ±0.5%. Hence, it was a forgone conclusion that, the present calculations were mesh size independent.

Table 2
The grid information for the models considered in this study.

	No. of nodes	No. of faces	No. of cells
P1-Model			
L-Mesh	103,792	215,612	111,820
H-Mesh	319,360	646,784	327,424
P2-Model			
L-Mesh	59,406	98,825	39,419
H-Mesh	284,016	448,748	164,732
P3-Model			
L-Mesh	65,249	107,702	42,453
H-Mesh	295,046	461,787	166,741

2.4. Boundary conditions

The flowing streams considered counter current while the inlet and outlet pressures chosen as the inlet and outlet boundary conditions; respectively. The heat exchanger length was chosen as 1 m, the entering flue gas and air temperatures were set fixed at 600 and 323 K, respectively. The boundary condition near the wall was double-edged coupled wall while for the rest of the places symmetry boundary conditions with respect to middle of the channel were implemented.

In order to simulate the turbulent stream through the plate heat exchanger, the K–ε with larger eddies model was utilised. The behaviour of this model near the wall was corrected by incorporating an enhanced wall treatment.

3. Modelling results

3.1. Temperature variations

In this study, the entering flue gas and air temperatures were set fixed at 600 and 323 K; respectively. Since the sulphuric acid dew point in the Tehran's refinery flue gas was around 400 K and it was intended to avoid the corrosion problem in this system, the safe operating temperature for the outlet flue gas was set at a minimum of 410 K [12]. Hence, the air flow passing through each of the P1–P3 models was variable. The flue gas and air temperature changes thru the length of all three types of the heat exchangers were displayed in Fig. 4. As indicated in this figure, utilizing the Chevron type plates resulted in 18% enhancement in the output air temperature.

3.2. Flow velocity

The flue gas velocity changes along the HE length for the three models demonstrated through the Fig. 5. As observed, through changing the plate from the flat (P1) to the Chevron (P2 and P3) geometry, considerable changes occurred in the gas velocity. The most alteration of velocity vectors took place in the P3 model possessing the highest Chevron angle. It is reiterated that, the P3 model possessed a smaller cross area for a given volume of gas to pass per unit time hence, a larger velocity was realized. Moreover, the higher Chevron angles of this model led to higher turbulent intensities considered next in this article.

3.3. Turbulence intensity

In Figs. 6 and 7 the turbulence intensity contours of the P2 and P3 models shown at the middle of the PHE (y = 0.5 m). The turbulence intensity parameter, I, indicated a measure of turbulence of a stream and defined as the ratio of absolute deviation of the velocity from its average value to this average velocity. This was given as a percentage by:

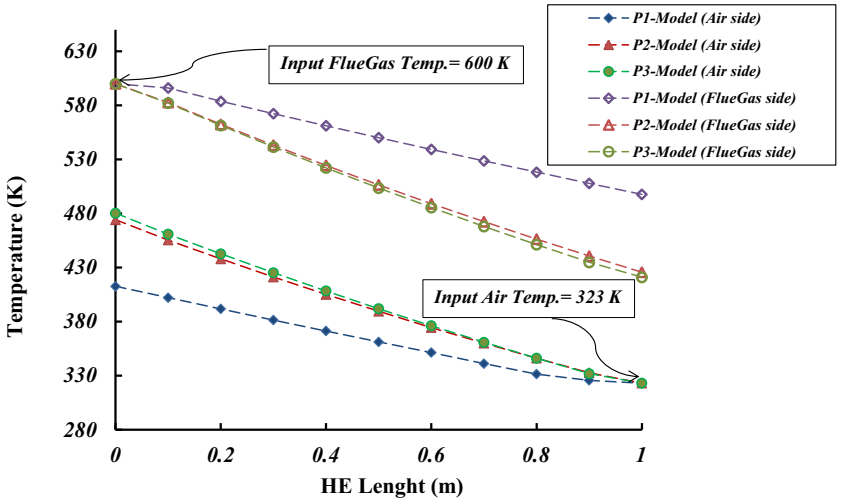

Fig. 4. Flue gas and air temperature changes vs. HE length for the three models developed in this study.

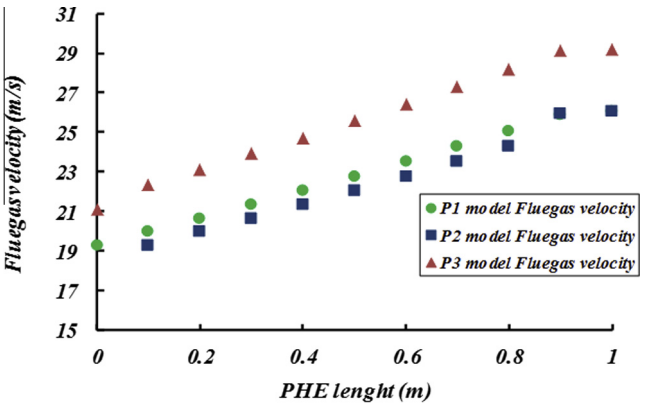

Fig. 5. Flue gas velocity along with the HE length.

$$I = |\overline{u} - u_{avg}|/u_{avg} * 100 \quad (10)$$

where $\overline{u}$ and u_{avg} indicated the actual and average velocities; respectively. Moreover, the average velocity was calculated through the following expression:

$$u_{avg} = \frac{\int_V |\vec{u}| dV}{V} \quad (11)$$

In which the V indicated the gas volume.

When comparing results of these two plate geometries, it is concluded that, with increasing of the Chevron angle (*i.e.*; from P2 to P3), variations of the distance between plates hence, their vacant space became more pronounced. This further attributed to sudden changes through the velocity vectors leading to higher velocity fluctuations thus, higher turbulence intensities. This latter phenomenon in turn caused enhanced heat transfer rate even though a higher pressure drop was also attained.

3.4. Fanning factor and pressure drop

In order to calculate the fanning factor and pressure drop, Eq. (4) was utilised. It is seen through contours of turbulence intensity and velocity, a decrease in Chevron angle caused lowering of a stream turbulence leading to a decrease in pressure drop between plates. This was also observed in previous studies [17,18]. The changes of the Flue gas pressure drop and outlet temperature versus the Chevron's angle calculated through this model were presented in Figs. 8 and 9. These figures reiterated the above findings that, as the Chevron angle increased, both the flue gas temperature changes with respect to its inlet value of the HE as well as; the total pressure drop through the HE length enhanced however, the raise in the total pressure drop was considerably more pronounced than the changes in the flue gas and air temperatures. This meant that, the total pressure drop's two folds effect should not be undermined or underestimated. In other words, it has to be accounted for as well as; taken seriously when choosing a PHE.

Through investigation of Fig. 10 it was apparent that the maximum fanning factor at Chevron type HEs took place in the P3 model. It is naturally expected that, the higher fanning factor resulted in geometries with higher turbulence intensity [15,17,18].

3.5. Nusselt number

According to the relation between the Nusselt and Reynolds numbers (Eq. (7)), it was expected that incrementing the latter led to enhancement of the former number [17,18]. Fig. 11 showed variations of the Nusselt with Reynolds number for all three aforementioned HE configurations.

As observed through Fig. 11, alterations of plates from the flat to Chevron geometries caused an increase in the Nusselt number hence, the heat transfer rate. Furthermore, comparison between the P2 and P3 geometries showed that, P3 geometry resulted in a greater heat transfer rate as well as; the Nusselt number. This was due to its higher turbulence intensity and maximum velocity compared with that of the P2 model.

Average values of the Nusselt number calculated for turbulent flow through different PHE's in this investigation, resulted in the following Dittus–Boelter correlations:

$$Nu = 0.823 Re^{0.46} Pr^{0.33}, R^2 = 0.9743 \quad (12)$$

$$Nu = 0.274 Re^{0.62} Pr^{0.33}, R^2 = 0.9480 \quad (13)$$

$$Nu = 0.062 Re^{0.84} Pr^{0.33}, R^2 = 0.9809 \quad (14)$$

For the flat PHE as well as; the Chevron types with 29° and 89°; respectively. These values indicated the new Nusselt number expressions developed for the gas–gas systems undertaken in the present study.

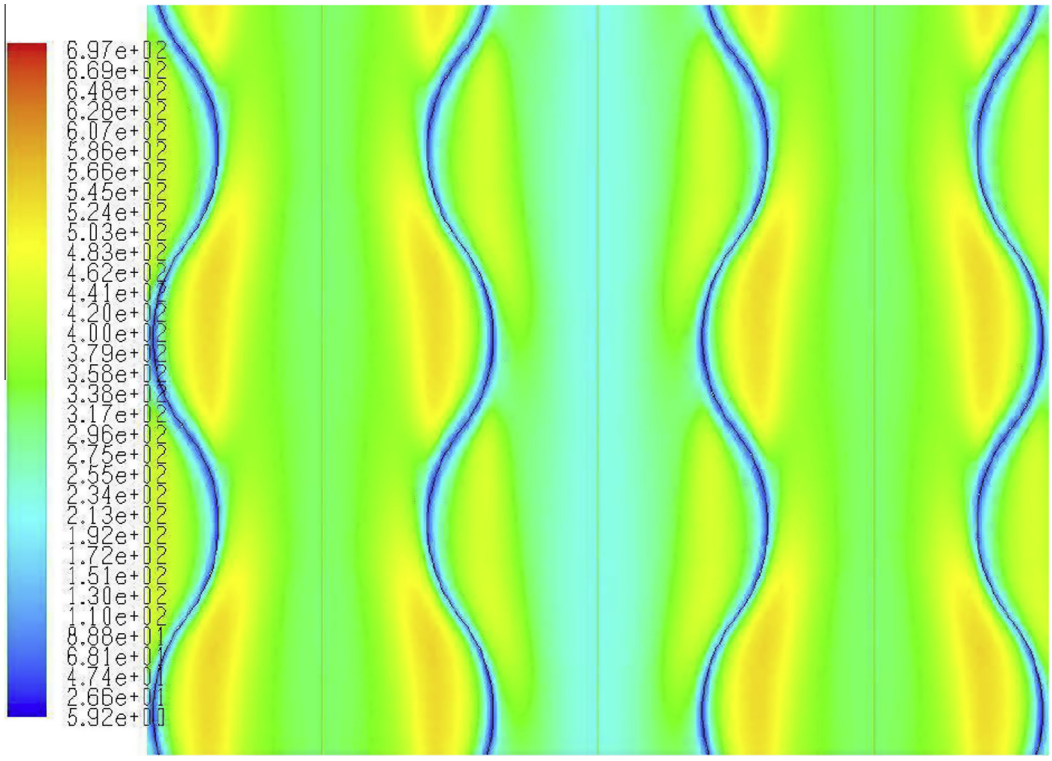

Fig. 6. The turbulence intensity contour for the P2 model.

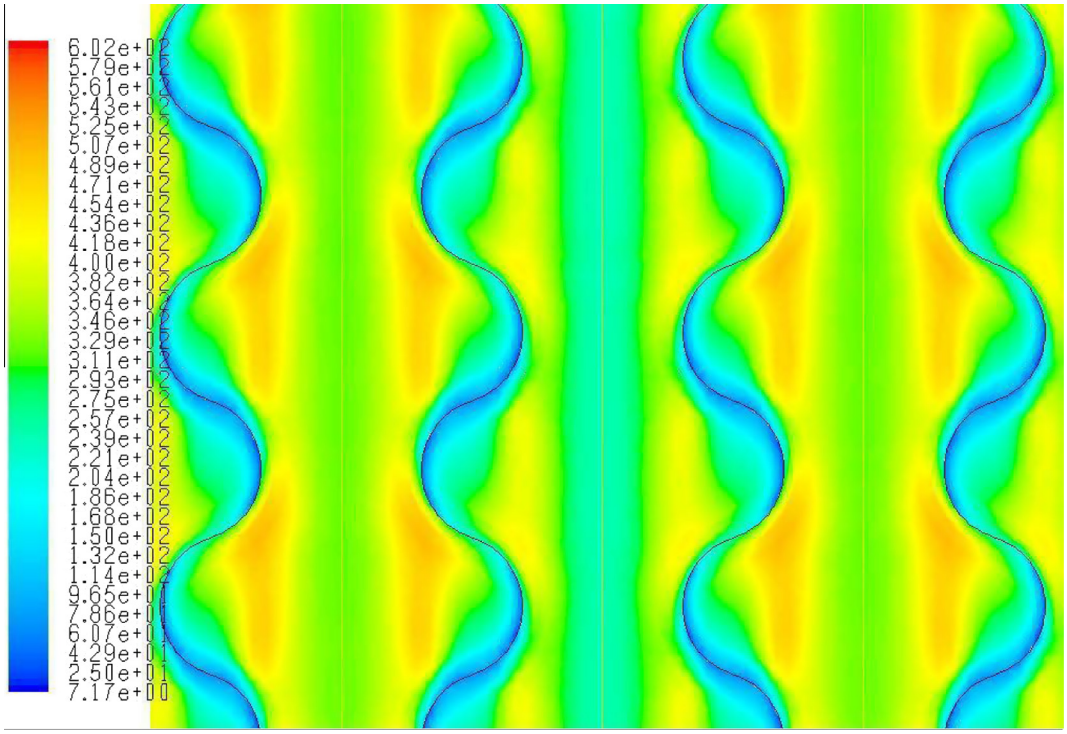

Fig. 7. The turbulence intensity contour for the P3 model.

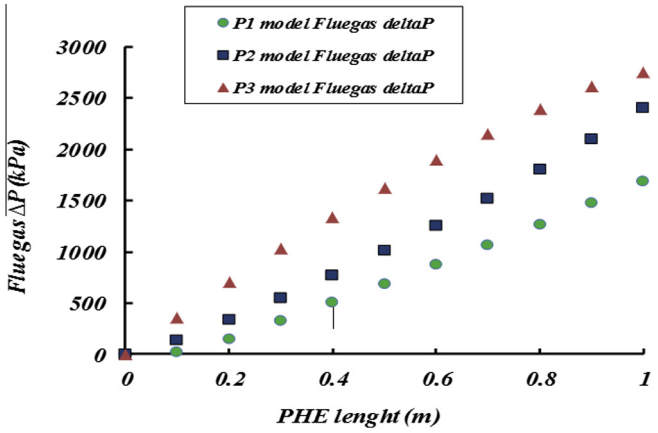

Fig. 8. Flue gas pressure drop along the HE length.

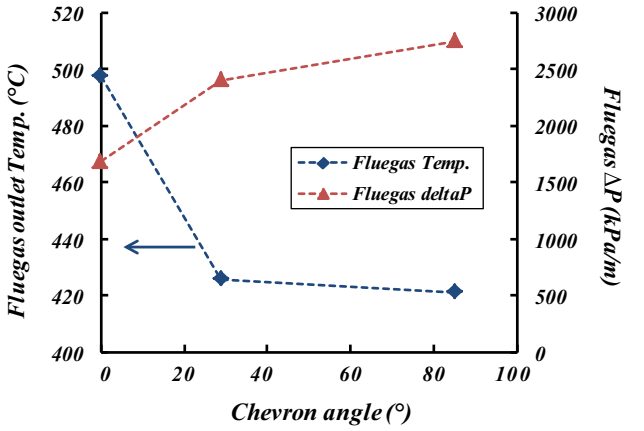

Fig. 9. Flue gas pressure drop and outlet temperature change versus Chevron angle predicted.

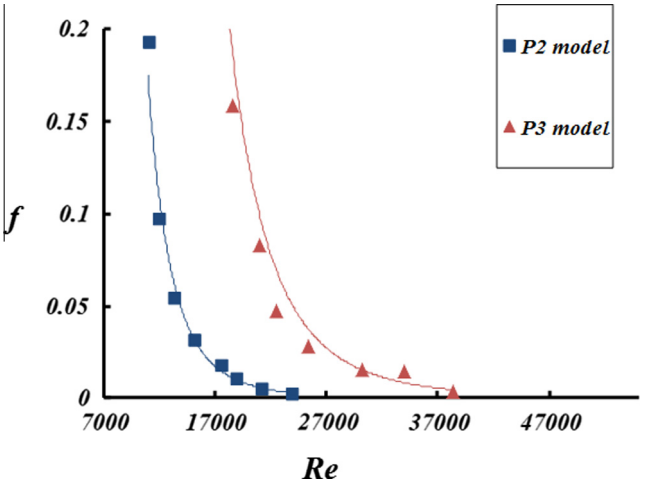

Fig. 10. The fanning factor versus Reynolds number.

4. Model validations

It is reminded that validations of the current models were based upon the correlations presented in Eqs. (12)–(14). In Figs. 12–14 comparison of present models' predictions with empirical data of others available in the open literature [1,19,20] were provided.

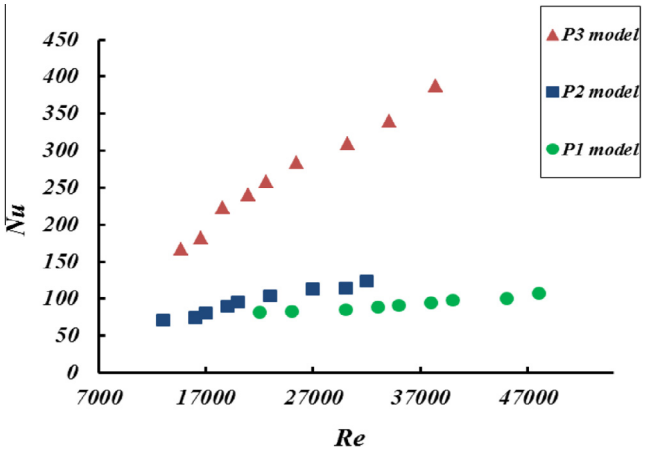

Fig. 11. Models' Nusselt versus Reynolds numbers predicted.

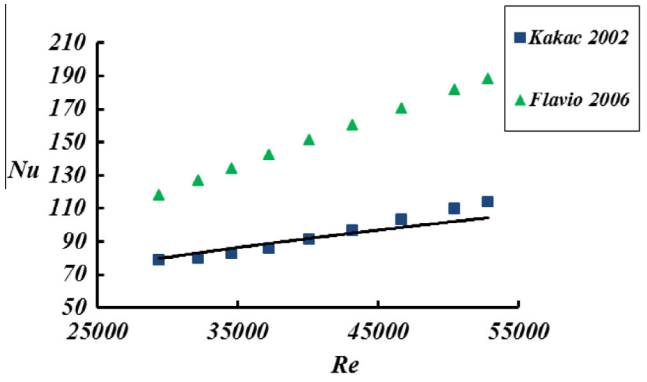

Fig. 12. The comparison of the P1 model predictions (solid line) with the empirical data (Flavio et al. [19]; Kakac and Liu [20]).

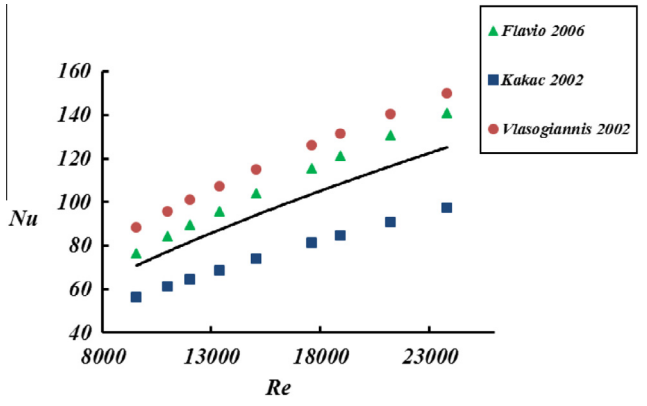

Fig. 13. The comparison of P2 model result (solid line) with empirical data (Vlasogiannis et al.[1]; Flavio et al. [19]; Kakac and Liu [20]).

It is noteworthy that, the data of the aforementioned references were for either liquid–liquid or liquid–gas HE systems as opposed to the ones understudied by the present models of the P1–P3 all of which were for the gas–gas systems. Furthermore, it is well accepted that, the heat transfer depended not only upon the HE's geometry but also, affected by the variations of the temperature dependent physical properties of the working fluids, the most important of which was the viscosity [15,16]. This meant that, since the gas and liquid viscosities changed quiet differently with the temperature variations, the respective heat transfer rates were

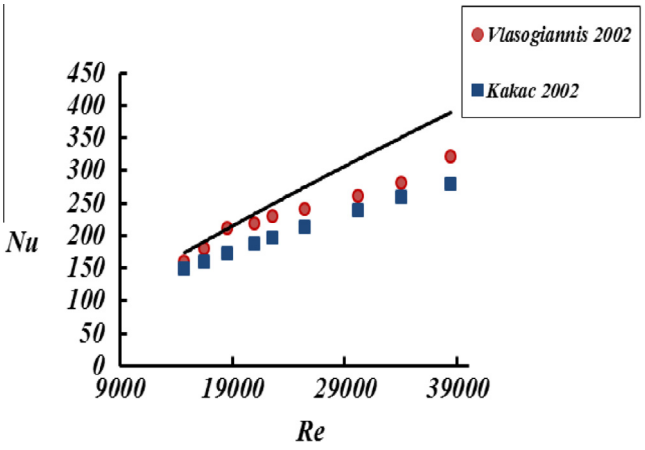

Fig. 14. The comparison of P3 model results (solid line) with empirical data (Vlasogiannis et al. [1]; Kakac and Liu [20]).

affected quite diversely leading to such comparisons. Therefore, a careful analysis of these comparisons was in order. In other words, one might better look at these comparisons in terms of; the theoretical models developed through this study predicted a correct pattern rather than close values when compared with the experimental data. Ultimately, it is admitted that due to unavailable experimental data with the same HE plate geometry and types of fluids used here, the reliability of the present models may not clearly be verified. Nonetheless, a maximum error of ±30% obtained amongst these data might still be considered promising.

5. Conclusion

The mathematical modelling of the flat and Chevron plate HEs clearly demonstrated the essential role of the Chevron angles upon the heat transfer rate and pressure drop. When the model changed from the flat (P1) to angular geometry of the Chevron plates (P2 and P3), the main alterations occurred in the velocity fluctuations hence, the turbulence intensities. The most pronounced changes occurred in the P3 model possessing the largest Chevron angle. Comparison between the two Chevron geometries showed that, whenever the Chevron angle became larger, the maximum flue gas velocity enhanced. In addition, comparison of these two Chevron models revealed that, the higher amount of the space available for the fluid flow due to the size of the Chevron's angle in turn; led to smaller turbulence intensity for the P2 model. This was due to a lower scattering of eddies occurring between plates for this configuration.

In all investigated models, an increased Reynolds number caused a decrease of the Fanning friction factor affecting the corresponding pressure drop. The maximum pressure drop and fanning factor appeared thru the P3 geometry. This was indicated by increasing of the turbulence within plates of this configuration. This pattern was further confirmed through comparison between the P1 and P2 models indicating the turbulence intensity of the P2 was greater than that of the P1 model also reported previously.

In all three aforementioned models, it was displayed that through increasing of the Reynolds number, the corresponding Nusselt number enhanced. Furthermore, by changing plates' geometry from the flat to Chevron a considerable increase in the Nusselt number as well as; heat transfer rate occurred. In addition, comparison between the P2 and P3 models also showed that, in the P3 geometry a larger heat transfer rate as well as, Nusselt number was resulted. This was attributed to a greater maximum velocity and turbulence intensity resulted from this model in comparison with those of the P2 configuration.

References

[1] P. Vlasogiannis, G. Karagiannis, P. Argyropoulos, V. Bontozoglou, Air–water two-phase flow and heat transfer in a plate heat exchanger, Int. J. Multiphase Flow 28 (2002) 757–772.
[2] F. Pinson, O. Gregoire, M. Quintard, M. Prat, O. Simonin, Modeling of turbulent heat transfer and thermal dispersion for flows in flat plate heat exchangers, Int. J. Heat Mass Transfer 50 (2007) 1500–1515.
[3] Yang Yujie, Li Yanzhong, Si Biao, Zheng Jieyu, Performance evaluation of heat transfer enhancement in plate-fin heat exchangers with offset strip fins, Physics Procedia 67 (2015) 543–550.
[4] Nur Rohmah, Ghalya Pikra, Andri Joko Purwanto, Rakhmad Indra Pramana, The effect of plate spacing in plate heat exchanger design as a condenser in organic Rankine cycle for low temperature heat source, Energy Procedia 68 (2015) 87–96.
[5] G. Jogi Nikhil, M. Lawankar Shailendra, Heat transfer analysis of corrugated plate heat exchanger of different plate geometry: a review, Int. J. Emerging Technol. Adv. Eng. 2 (2012) 110–115.
[6] O. Arsenyeva, P. Kapustenko, L. Tovazhnyanskyy, G. Khavin, The influence of plate corrugations geometry on plate heat exchanger performance in specified process conditions, J. Energy 57 (2013) 201–207.
[7] M. Goodarzi, S. Mazharmanesh, Heat transfer enhancement in parallel-plate double-pass heat exchanger using sinusoidal separating plate, Int. J. Therm. Sci. 72 (2013) 115–124.
[8] Oana Giurgiu, Angela Pleşa, Lavinia Socaciu, Plate heat exchangers – flow analysis through mini channels, J. Energy Procedia 85 (2016) 244–251.
[9] Sassan Etemad, Bengt Sundén, Hydraulic and thermal simulations of a cross-corrugated plate heat exchanger unitary cell, J. Heat Transfer Eng. (2016) 475–486.
[10] Emanuel Feru, Bram de Jager, Frank Willems, Maarten Steinbuch, Two phase plate-fin heat exchanger modeling for waste heat recovery system in diesel engines, J. Appl. Energy 133 (2014) 183–196.
[11] L. Zhi-jian, Z. Guan-min, T. Mao-cheng, F. Ming-xiu, Flow resistance and heat transfer characteristic of a new-type plate heat exchanger, J. Hydrodyn. 20 (2008) 524–529.
[12] B. ZareNezhad, A. Aminian, A multi-layer feed forward neural network model for accurate prediction of flue gas sulphuric acid dew points in process industry, Appl. Therm. Eng. 30 (2010) 692–696.
[13] Y.C. Wang, G.H. Tang, Prediction of Sulfuric acid dew point temperature on heat transfer fin surface, Appl. Therm. Eng. 98 (2016) 492–501.
[14] C. Fernandes, R. Dias, J. Nobrega, J. Maia, Laminar flow in Chevron-type plate heat exchangers: CFD analysis of tortuosity, shape factor and friction factor, Chem. Eng. Process. 46 (2007) 825–833.
[15] X. Shi, D. Che, B. Agnew, J. Gao, An investigation of the performance of compact heat exchanger for latent heat recovery from exhaust flue gases, Int. J. Heat Mass Transfer 54 (2011) 606–615.
[16] C. Fernandes, R. Dias, J. Nobrega, J. Maia, Effect of corrugation angle on the thermal behaviour of power-law fluids during a flow in plate heat exchangers, Proceeding of Fifth International Conference on Enhanced, Compact and Ultra-Compact Heat Exchangers: Science,, Engineering and Technology, USA, 2005.
[17] D. Dović, B. Palm, S. Švaić, Generalized correlations for predicting heat transfer and pressure drop in plate heat exchanger channels of arbitrary geometry, Int. J. Heat Mass Transfer 52 (2009) 4553–4563.
[18] F. Elshafei, M. Awad, E. El-Negiry, A. Ali, Heat transfer and pressure drop in corrugated channels, Energy 35 (2010) 101–110.
[19] C. Flavio, C. Galeazzoa, R. Miurab, A. Jorge, C. Tadini, Experimental and numerical heat transfer in a plate heat exchanger, Chem. Eng. Sci. 61 (2006) 7133–7138.
[20] S. Kakac, H. Liu, Heat Exchangers: Selection, Rating and Thermal Design, CRC Press, 2002. 373–412.